International Journal of Medical Microbiology 309 (2019) 151324

Contents lists available at ScienceDirect

International Journal of Medical Microbiology

journal homepage: www.elsevier.com/locate/ijmm

The multicopper oxidase of *Mycobacterium tuberculosis* (MmcO) exhibits ferroxidase activity and scavenges reactive oxygen species in activated THP-1 cells

Eyad Kinkar, Ayat Kinkar, Mazen Saleh*

Department of Biology, Laurentian University, Sudbury, Ontario, P3E 2C6, Canada

ARTICLE INFO

Keywords:
Mycobacterium tuberculosis
Multicopper oxidase
ROS
THP-1
Ferroxidase

ABSTRACT

The MmcO protein of *Mycobacterium tuberculosis* is a membrane-associated multicopper oxidase. Its natural substrate(s) and its role in pathogenesis are not well characterized. A recent report proposes that MmcO contributes to copper resistance in *M. tuberculosis* during infection. We have expressed and reconstituted the active enzyme from inclusion bodies in *E. coli*. MmcO exhibits maximal activity against the experimental substrate 2,2′-azino-bis (3-ethylbenzothiazoline-6-sulphonic acid) or ABTS, at pH 4. The enzyme also exhibits ferroxidase activity at pH 4. Most notable was the finding that MmcO is able to scavenge the reactive oxygen species (ROS) generated by the xanthine/xanthine oxidase enzyme system. This ROS scavenging activity of MmcO was also evident against ROS generated by THP-1 cells. We propose that MmcO protects *M. tuberculosis* during infection against ROS attack in addition to providing copper resistance to the pathogen.

1. Introduction

The multicopper oxidases, also known as blue oxidases, contain a multicopper center and oxidize using molecular oxygen from a variety of substrates. This class of enzymes include the laccase (EC1.10.3.2), the ascorbate oxidase (EC 1.9.3.1), and the ferroxidase ceruplasmin (EC 1.16.3.1) plus others (Messerschmidt and Huber, 1990). Representatives of this class of enzymes serve a number of physiological roles including iron acquisition in *P. aeruginosa* (Huston et al., 2002), copper tolerance (Grass and Rensing, 2001), oxidation of phenolate siderophore in *E. coli* (Kim et al., 2001), and oxidation of manganese in a number of marine *Bacillus* species (Dick et al., 2008). In humans, ceruplasmin oxidizes norepinephrine and serotonin (Young and Curzon, 1972), displays NO-oxidase/NO_2^- synthase (Shiva et al., 2006), glutathione-dependent peroxidase (Park et al., 1999), and superoxide dismutase (Vasil'ev et al., 1988) activities.

The *M. tuberculosis* MmcO preprotein (Rv 0846c) is 505 amino acids long. It contains a typical twin-arginine (TAT) N-terminal signal sequence similar to multicopper oxidases of *Pseudomonas*, *Klebsiella*, and *Bordetella* (Huston et al., 2002). The cysteine at position 35 in the N-terminus follows a potential signal peptidase cleavage site (LAA) and is the likely site of lipid modification that anchors the protein to the membrane. A recent study by Rowland and Niederweis (2013) have shown that this putative lipidation site is not required for activity of the enzyme. The authors also demonstrated that an mmcO deletion mutant lacks whole cell lysate ferroxidase activity and shows reduced resistance to copper toxicity.

Multicopper oxidases may also have physiological roles related to oxidative stress. Sensitivity to copper in a cueO mutant of *E. coli* has been shown to be related to oxidative stress (Tree et al., 2007). The salivary antigen-5/CAP family members of *Dipetalogaaster maxima* and *Triatoma infestans* exhibit antioxidant activities and inhibit the oxidative burst in Neutrophils (Assumpção et al., 2013). To explore possible similar activity by MmcO, we have cloned and expressed the protein in *E. coli*. The enzyme was reconstituted from inclusion bodies and characterized copper binding of the protein by following changes in the protein's absorption spectrum upon addition of copper. The reconstituted enzyme showed ferroxidase activity, confirming the results of cell lysate experiments from Rowland and Niederweis (2013). MmcO displayed scavenging activity against ROS generated in the xanthine-xanthine oxidase enzyme system but most importantly its ability to scavenge ROS generated in activated THP-1 cell.

Abbreviations: ROS, reactive oxygen species; MmcO, the multicopper oxidase of *Mycobacterium tuberculosis*; ABTS, 22'-azino-bis(3-ethylbenzothiazoline-6-sulphonic acid); PMA, phorbol 12-myristate 13-acetate; PCR, polymerase chain reaction; PMSF, phenyl methane sulfonyl fluoride; PVDF, polyvinylidene difluoride

* Corresponding author.
E-mail address: msaleh@laurentian.ca (M. Saleh).

https://doi.org/10.1016/j.ijmm.2019.06.004
Received 21 March 2019; Received in revised form 29 May 2019; Accepted 22 June 2019

2. Materials and methods

2.1. Materials

The *E. coli* expression vector pET21and anti-6xHis antibodies was purchased from GenScript (Piscataway, NJ). Restriction enzymes NdeI and NotI, BL-21 cells, dNTP's, and Q5 High fidelity Taq polymerase were purchased from New England Biolabs, Inc. (Ipswich, MA). *M. tuberculosis* genomic DNA were provided by the Biodefense and Emerging Infections Research Resources Repository (Manassas, VA). THP-1 cells were purchased from ATCC. Isopropyl β-D-1-thiogalactopyranoside (IPTG), ABTS (2,2′-azino-bis-3-ethylbenzthiazoline-6-sulphonic acid) substrate, phorbol 12-myristate 13-acetate (PMA), and Streptolysin-O were purchased from Sigma-Aldrich Canada Co. (Oakville, ON). Unless otherwise indicated, all other reagents were also purchased from Sigma-Aldrich Canada Co. (Oakville, ON).

2.2. Bioinformatics

Using Multalin (Corpet, 1988), the amino acid sequence of MmcO (Rv0846c) was aligned with those of the laccase-like multicopper oxidase from *Aspergillus niger* (MmcG) and the multicopper oxidase from *Campylobacter jejuni* (CueO). Their accession numbers are 5LWX-A and PKD36697.1, respectively. The 3D model of MmcO was simulated based on homology (31% identity) to the CueO of *Campylobacter jejuni* (Silva et al., 2012) [accession #: Pdb3ZX1] using the Protein Model Portal (Haas et al., 2013) and visualized using the NGL viewer (Rose and Hildebrand, 2015).

2.3. Cloning and expression of mmcO

The forward primer 5′ **AATAAT***GATCTC*ATGCCCGAGCTGGCCACG 3′] and the reverse primer 5′ **AATAAT***CGCCGGCG*CGGCGGCGGCGG CCCCAGAATGTAGTCCAG 3′ were used to amplify *mmcO* from *M. tuberculosis* genomic DNA. Both of these primers contain restriction sites (red, for NdeI and NotI), overhang nucleotides (bolded black), and a linker (blue). The primers were synthesised by Thermo Fisher Scientific (Waltham, MA). The translated PCR product contains a 6xHis tag (C-terminal) separated from the protein by a 9xGly linker (part of the pET21a vector). The first 34 codons in the gene (coding for a potential TAT signal sequence) were removed and the Cys at position 35 was changed to a start codon. The PCR product was cloned into pET21a using the NdeI/NotI restriction sites using DNA ligase and supplier's instructions (Thermo Fisher Scientific, Waltham, MA). The modified vector thus produced (pET21a-*mmcO*) was used for expression of the protein. Sequence of the PCR product was confirmed by sequencing at the Centre for Applied Genomics at Sick Kids Hospital (Toronto, ON).

2.4. Extraction and refolding of MmcO

Analysis of expression of MmcO revealed that the protein aggregates within inclusion bodies in *E. coli*. The extraction of the recombinant protein from inclusion bodies was based on the protocol of Rudolph and Lilie (Rudolph and Lilie, 1996). Briefly, harvested cells were re-suspended in 10 mls lysis buffer [50 mM Tris − HCl pH 7.5 containing 8 M Urea, 1.0 mM phenyl methane sulfonyl fluoride (PMSF) (v/v), and 5 mM dithiothreitol. The suspension was sonicated 10 cycles at 16 V using a W208 Sonicator (Heat Systems UltraSonic Inc.) equipped with a micro tip. Each cycle consisted of 5 s on followed by a 30 s rest on ice. The resulting suspension was centrifuged at 4800 xg [Eppendorf Centrifuge 5804 R, Brinkman Instruments. Inc] and 4 °C for 35 min. Several strategies were investigated to maximize the refolding of active MmcO. Dilution of the extract into large volumes of Tris or Acetate buffers of various pH levels and NaCl, copper sulfate, and glycerol concentrations were investigated. Direct dilution into 500x (v/v) 50 mM Tris, pH 7.4 containing 100 mM NaCl provided some of the highest recoveries of active enzyme. Slow refolding within dialysis tubing against this same buffer also provided comparatively high yield of active enzyme (data not shown). The dialysis method was subsequently adopted to produce the active enzyme for this project. Briefly, the supernatant of the extract was transferred to dialysis tubing (3500 Daltons cut-off) and subjected to dialysis against 500 ml of 50 mM Tris − HCl pH 7.4 containing 100 mM NaCl. The dialysis was performed at ambient temperature for 4 h. The dialysis buffer was replaced with fresh buffer and dialysis was continued over night at 4 °C.

2.5. Nickel affinity chromatography

The purification of the recombinant His-tagged MmcO protein was carried out using a 1.0 mL Nickel column (GE Healthcare) according to manufacturer's instructions. The refolded protein was first desalted on a HiPrep 26/10 desalting column (GE Healthcare) in 20 mM phosphate buffer, pH 7.4 containing 0.5 M NaCl and 25 mM Imidazole (Nickel binding buffer). This buffer exchange allows for direct application of the sample onto the Nickel column. The desalted extract was applied at a flow rate of 1 ml /min followed by washing with 20 column volumes of binding buffer. The bound protein was eluted in 10 column volume of elution buffer (20 mM phosphate buffer, pH 7.4 containing 0.5 M NaCl and 500 mM imidazole). The eluted protein was finally dialyzed against 1.0 L of 10 mM phosphate buffer, pH 7.4 and stored for subsequent testing.

2.6. Sodium dodecyl sulfate polyacrylamide gel electrophoresis (SDS-PAGE) and western blot

Protein extracts were separated on 10% SDS-PAGE gels under denaturing conditions. The gels were subjected to electrophoresis for 45 min at a constant voltage of 100 V using a Mini-PROTEAN Tetra System (Bio-Rad Laboratories, Hercules, CA) and visualized by staining with Coomassie brilliant blue R-250. For western blots, the proteins were transferred onto a PVDF membrane using a semi-dry apparatus (Bio-Rad Trans-Blot) at constant voltage (15 V) for 30 min. The membrane was subsequently blocked by incubation in blocking solution (5% skim milk in 1X PBST buffer contains 8 g/L NaCl, 0.2 g/L KCl, 1.44 g/L Na_2HPO_4, 0.24 g/L KH_2PO_4 and 0.05% Tween-20) at 4 °C with shaking for 12 h. This membrane was rinsed 3 times in 1 X PBST and then probed by incubation with the primary anti-His-tag antibody at a 1:3000 dilution in 5% milk in 1 X PBST at RT with shaking for 2 h. Following washing in PBST, the membrane was finally probed with anti-rabbit IgG-alkaline phosphatase conjugated antibody (Biomeda Corp., Foster City, CA) at 1:30000 dilution at RT with shaking for 2 h. Bound antibodies were detected using BCIP/NBT reagents [0.8 mg 5-bromo-4-chloro-3-indolyl phosphate and 1.2 mg nitro blue tetrazolium in 10 ml of detection buffer (50 mM Tris − HCl pH 9.6, 5 mM $MgCl_2$)].

2.7. ABTS assay

The MmcO activity assay was based on the oxidation of ABTS (2,2′-azino-bis-3-ethylbenzthiazoline-6-sulphonic acid) as described by Park et al. (1999) with modifications. Briefly, the assay was carried out in 50 mM sodium acetate buffer, pH 4 containing 2 mM ABTS and 2 mM $CuSO_4$. Reaction were incubated at RT with shaking for 2 h. Reactions were followed at 405 nm and specific activity was calculated using a molar absorptivity coefficient $\varepsilon = 18{,}400\ M^{-1}\,cm^{-1}$. For determination of reaction pH optima, the pH of the acetate buffer was adjusted or the acetate was replaced with Tris to get the desired pH.

2.8. Ferroxidase assay

Ferroxidase activity of the refolded MmcO protein was assessed by following the conversion of Fe (II) to Fe (III). The conversion is accompanied by an increase in absorbance at 315 nm and the assay

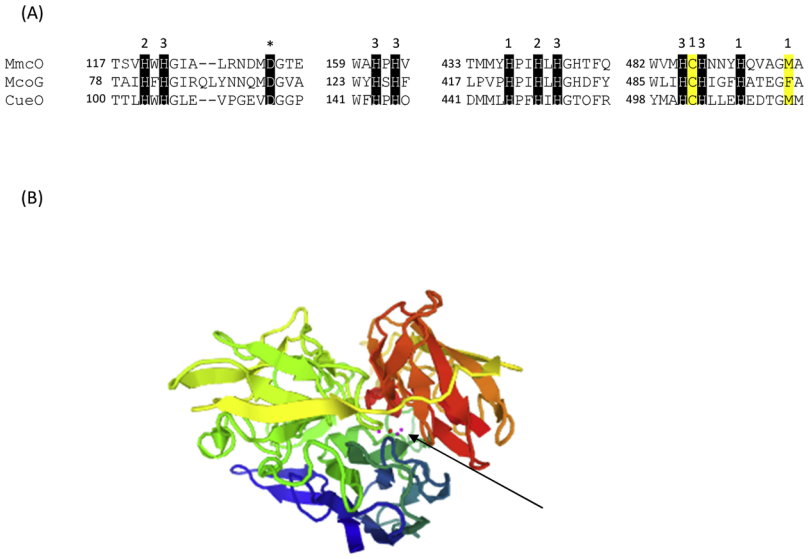

Fig. 1. (A) Sequence alignment of MmcO, McoG, and CueO. Only the regions containing the copper ligating His are shown. The numbers above each His denotes the type of copper that the amino acid chelates (type 1, type 2, or type 3). The conserved Asp (*) is proposed to be involved in the enzymatic reaction (proton donation). (B) Proposed model of MmcO based on homology to the multicopper oxidase of *Campylobacter jejuni* (CueO). Copper atoms are shown in violet colour (arrow) (For interpretation of the references to colour in this figure legend, the reader is referred to the web version of this article).

followed the protocol of Bonomi et al. (1996). In a total reaction volume of 1.0 ml, 50 mM HEPES buffer (pH 7.0) was mixed with ferrous ammonium sulfate (2 mM final concentration) and 50 µg of refolded MmcO protein at ambient temperature. Upon mixing of the components, the spectra were immediately collected on a HITACHI U-3000 spectrophotometer.

2.9. Xanthine oxidase-luminol assay

Reactions were assembled in a total reaction volume of 200 µl according to the protocol of Assumpção et al. (2013) with minor modifications. Reactions contained 50 mM phosphate-buffered saline (pH 7.4), 2 mM hypoxanthine, 0.1 mM luminol, and various amounts of refolded MmcO protein. The reactions were initiated by the addition of 1 milliunit xanthine oxidase and the reactions immediately followed in a Packard LumiCount luminometer.

2.10. ROS production and detection in THP-1 cells

THP-1 cells were cultured as described by Walev et al. (2001) with some modifications. In brief, cells were cultured in Corning® T75 flasks in GI1640 Medium [Hyclone] with 10% Fetal Calf Serum (FCS), 100 µg/ml streptomycin, and 100 unit/ml penicillin at 37 °C and 5% CO_2. Cell viability was monitored using Trypan Blue staining. Live cells (~9×10^6) in 200 µl were permeated using 20 ng/ml Streptolysin-O in the presence of 50 µg/ml Fluorescein Isothiocyanate Conjugated (FITC)-albumin. Prior to use, SLO was activated by incubation in activation buffer (20 mM N-2-hydroxyethyl piperazine-*N*-2-ethanesulfonic acid (HEPES), pH 7.2 containing 20 mM DTT) at 37 °C for 10 min. In test samples, MmcO in various amounts was included in the permeabilization reactions. Following permeabilization, the pores were sealed by addition of ice cold RPMI media supplemented with 10% FCS, 2 mM $CaCl_2$, 100 µg/ml streptomycin, and 100 unit/ml penicillin before being placed back at 37 °C and 5% CO_2. Permeabilization and resealing of the cells was confirmed using confocal microscopy to follow the FITC-BSA used in the reactions. The ROS assay was carried out using ROS-Glo™ H_2O_2 Assay kit (Promega Corp.). This assay is based on the Luciferase/luciferin system and luminescence levels in the reactions reflect the amount of produced ROS. Reactions were carried out in triplicates in 100 µl volumes as described by the manufacturer. ROS production was initiated by treatment of the cells with 50 ng/ml phorbol 12-myristate 13-acetate (PMA). ROS production was followed using a Synergy H4 Luminescence reader for 20 min.

2.11. Flow cytometry

THP-1 cells (1×10^6) were seeded in 6-well plate and incubated until 80–90% confluency in complete medium at 37 °C, 5% CO_2. Following incubation, cells were permeabilized using 20 ng/ml Streptolysin-O (SLO) [Sigma-Aldrich] then MmcO (125 ng/ml, 250 ng/ml, or 500 ng/ml) in serum free GI-1640 Medium [Hyclone] was added and the cultures mixed for 15 min. Cells were washed two times with serum free GI media followed by resuspension in 3 ml of serum free GI media. Permeabilized cells were sealed by replacing the media with ice cold RPMI media supplemented with 10% FCS, 100 µg/ml streptomycin, 100 unit/ml penicillin, and 2 mM CaCl2. The samples were then incubated at 37 °C, 5% CO_2 for a further 1 h period. The samples were subsequently collected and resuspended in 2 ml of serum free RPMI media. After that cells were incubated with 50 ng/ml phorbol 12-myristate 13-acetate (PMA) as the ROS inducer and stained with deep red [Cellular ROS Assay Kit (Deep Red) from Abcam, Cambridge, MA, USA]. Cells were sorted and counted using the BD FACSCanto™ II flow cytometer (BD Biosciences, CA, USA). Fluorescence intensity at Ex/m = 650/675 nm was used for cell analysis.

3. Results

3.1. MmcO structure

Sequence alignment of MmcO with two homologous proteins, the laccase-like multicopper oxidase from *Aspergillus niger* (MmcG) and the multicopper oxidase from *Campylobacter jejuni* (CueO), shows conservation of sequences flanking the conserved histidines and the aspartic acid involved in the oxidation of substrates (Fig. 1A). The histidines in MmcO are His120, 122, 161, 163, 437, 440, 442, 485, 487, and 491. Simulation of the 3D structure of MmcO shows a characteristic Greek key β-barrel topology with three distinct cupredoxin-type domains (Silva et al., 2012). Chelated copper ions (Fig. 1B) make up a mononuclear type 1 copper center and a trinuclear cluster of two type 3 and one type 2 copper atoms.

3.2. Purified MmcO binds copper

Upon induction of *E. coli* BL-21 harboring the mmcO plasmid a strong band at approximately 56 kDa appears in the pellet fraction of extracted cells (Fig. 2, panel A, lane 3). This pellet fraction corresponds to inclusion bodies and shows a relatively simple band pattern typical of inclusion bodies. The identity of the protein in this band was

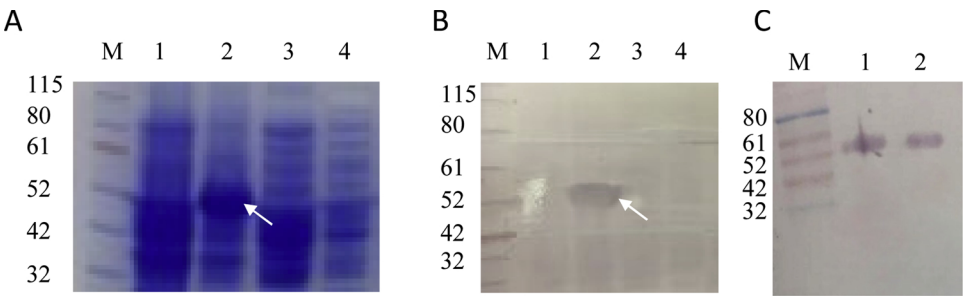

Fig. 2. Purification of expressed MmcO. Panel A shows the Coomassie-stained SDS-PAGE gel. Lanes: M, protein marker; 1, pellet extract of BL-21 harbouring the pET-mmcO vector before induction; 2, pellet extract of BL-21 harbouring the pET-mmcO vector after induction; 3, membrane fraction of BL-21 harbouring the pET-mmcO vector after induction; and 4, cytoplasmic fraction of BL-21 harbouring the pET-mmcO vector after induction. Panel B shows the corresponding western blot developed with ani-6xHis tag antibodies. The band at approximately 55 kDa (arrows) corresponds to MmcO. Panel C is a western blot of purified MmcO before (lane 1) and after (lane 2) refolding.

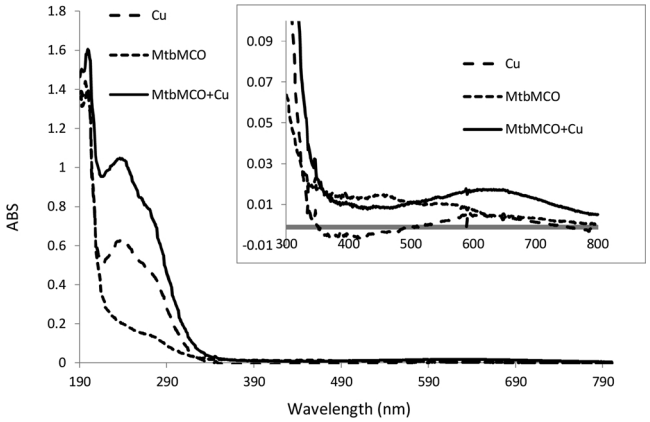

Fig. 3. Absorption spectrum of purified and refolded MmcO before and after the addition of $CuSo_4$. Inset shows the typical maximum at about 610 nm.

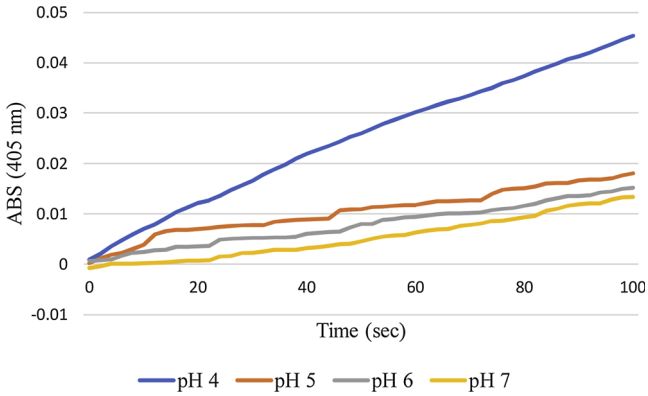

Fig. 4. pH dependence of MmcO oxidase activity against ABTS. The reaction time course at each pH indicated in the figure is a single time course and represent typical experiments.

confirmed by in-gel tryptic digest and mass spectrometry and as well as anti-6xHis antibody reactivity (Fig. 2, panel B, lane 3). Following purification with the nickel affinity resin a homogenous band representing MmcO was obtained (Fig. 2, panel C, lanes 1 and 2). Multicopper oxidases, including those with ferroxidase activity, bind copper *in vitro* accompanied with distinctive spectral changes. The most prominent spectral feature of purified MmcO is an absorption band between 610–640 nm. There is also a shoulder at about 330 nm. The former is due to binding to copper in a copper type 1 [Cu (II)] binding center (Sakurai and Kataoka, 2007; Hassett et al., 1998). When mixed with Cu (II), purified MmcO displays similar changes in its absorption spectrum (Fig. 3) to those observed in other [Cu (II)]-binding proteins such as the Fet3 multicopper ferroxidase (Hassett et al., 1998). These characteristic spectral features have also been reported for CueO multicopper oxidase, bilirubin oxidase, and laccase (Sakurai and Kataoka, 2007). This result was an indication that the purified MmcO was refolded properly and that the oxidase activity against ABTS in our assays were due to active MmcO.

3.3. pH-dependence of purified MmcO activity against ABTS

The ABTS enzyme substrate used to follow the activity of purified MmcO is the substrate of choice for oxidases and laccases. The assay is performed at acidic pH as this has been established as the optimum reaction pH in the literature. Activity of MmcO was evaluated for its dependence on pH to confirm the applicability of this rule. From the initial rate of reaction, MmcO activity was observed to increase as the pH became more and more acidic (Fig. 4). Maximal activity was observed at pH 4.0.

3.4. Purified MmcO displays ferroxidase activity

A number of multicopper oxidases exhibit ferroxidase activity. These include, but are not limited to, Ceruloplasmin in humans and Fet3 in *S. cerevisiae* (Frieden and Hsieh, 1976), and PcoA of *P. aeruginosa* (Huston et al., 2002). Ferroxidase activity has also been associated with MmcO as the ΔmmcO mutant of *M. tuberculosis* showed significantly reduced activity, as was the oxidase activity (Rowland and Niederweis, 2013). Our results (Fig. 5) confirm that the observed ferroxidase and oxidase activities associated with whole cells or fractions of whole cells of *M. tuberculosis* reported by Rowland and Niederweis (2013) are due to MmcO. Activity of MmcO has been proposed to contribute to copper homeostasis in *M. tuberculosis* as the ΔmmcO

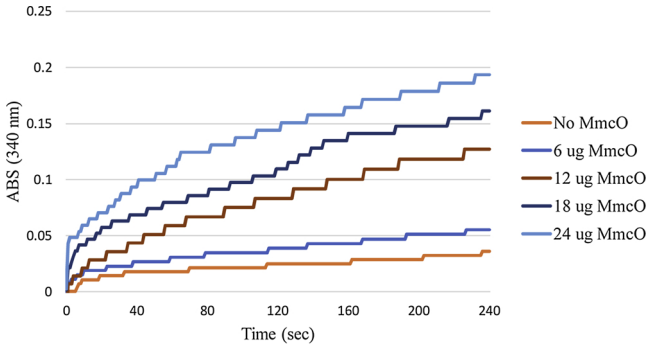

Fig. 5. Ferroxidase activity of MmcO. Pre-assembled reactions were initiated by the addition of ferrous ammonium sulfate (2 mM final concentration), followed immediately by absorbance measurements at 305 nm. The reaction time course at each MmcO concentration indicated in the figure is a single rime course and represents typical experiments.

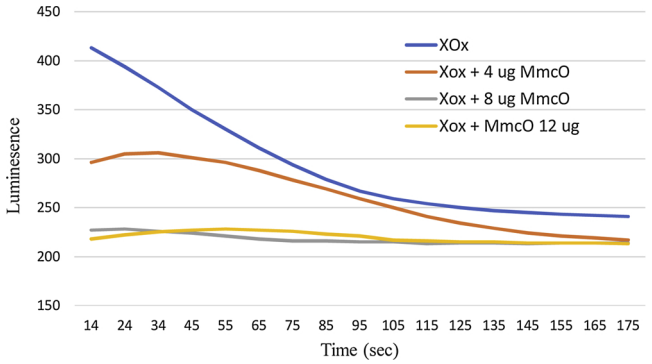

Fig. 6. Suppression of ROS produced in the xanthine/xanthine oxidase assay. Xox represents xanthine oxidase. Pre-assembled reactions were initiated by the addition of MmcO, followed immediately by luminescence measurements. The reaction time course at each MmcO concentration indicated in the figure is a single time course and represents typical experiments.

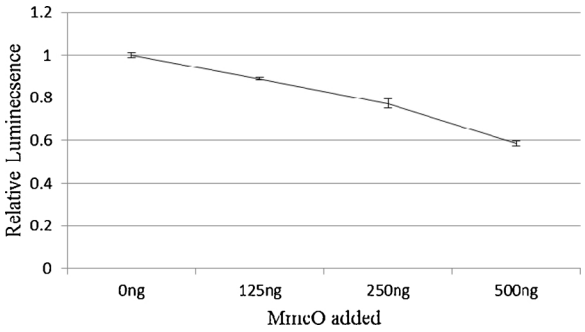

Fig. 7. ROS scavenging activity of MmcO in THP-1 cells. THP-1 cells were loaded with MmcO and induced with PMA (at 50 ng/ml final concentration) for ROS production. Bar values represent the mean ± SE. ROS released from THP-1 cells were determined indirectly by changes in the luminescence of lucigenin. Values represent the mean of triplicate measurements and the asterisks indicate statistical significance at $p < 0.05$.

mutant showed increased sensitivity to copper toxicity (Rowland and Niederweis (2013). Ferroxidase activity implicates MmcO as also contributing to iron homeostasis.

3.5. MmcO suppresses ROS production in vitro

The xanthine oxidase assay produces O_2 as a reaction by-product. In the presence of an appropriate detector, such as luminol, relative levels of this ROS can be determined. When MmcO is present in the reaction, luminescence levels decrease in a dose-dependent manner (Fig. 6). This is clear indication that MmcO can suppress the release of ROS produced in this reaction system. This Cu^{2+}-dependent antioxidant activity of Cu (II)-containing enzymes was also reported for salivary antigen-5/CAP family members from the hematophagous insects *Dipetalogaster maxima* and *Triatoma infestans* (Assumpção et al., 2013). Those enzymes exhibit a variety of physiological effects, including the inhibition of collagen-induced platelet aggregation and inhibition of the neutrophil respiratory burst (Assumpção et al., 2013). The latter effect is of particular interest in *M. tuberculosis* infections. This prompted us to look at the antioxidant activity of MmcO in similar cells known to be involved in immune defense during *M. tuberculosis* infections.

3.6. MmcO suppresses ROS production in THP-1 cells

THP-1 cells were used to investigate ROS production and effects of MmcO thereon. Purified MmcO was loaded into to the THP-1 cells using Streptolysin O to facilitate membrane permeability. THP-1 cells were treated with Phorbol 12-myristate 13-acetate (PMA) to promote ROS production in this assay system. Interestingly, we found that when we exposed the PMA-induced THP-1 cells to the purified MmcO, the levels of ROS detected were reduced in a dose-dependent manner (Fig. 7). A significant reduction in the amount of detected ROS was observed when MmcO was present (at 500 ng) in the reaction, reducing the ROS levels to 59% of the control. To confirm these results, a similar experiment was carried out but the produced ROS by THP-1 cells in the presence or absence of MmcO was detected using the deep red fluorescent dye and cell sorting. Detected ROS from activated THP-1 cells showed dose-dependent reduction in the presence of MmcO (Table 1). At 500 ng of refolded MmcO, only 38% (compared to the control) of released ROS could be detected under those conditions.

Table 1
Effect of MmcO on the release of ROS upon activation of THP-1 cells with PMA. THP-1 cells, having MmcO incorporated within the cytoplasm, were activated by treatment with PMA (50 ng/ml) and ROS produced were detected by Deep Red fluorescence (Abcam) using flow cytometry.

MmcO added (ng)	Relative Fluorescence	± SE
0	1	0.01
125	0.98	0.007
250	0.49	0.02
500	0.38	0.01

4. Discussion

Pathogenic mycobacteria is a successful intracellular pathogen due to two aspects of its physiology: its ability to evade certain immune responses and its ability to protect itself from those responses that it is unable to evade (Longhi et al., 2016; Hmama et al., 2015). The former reflects the ability of the pathogen to attenuate intracellular events in phagocytic cells following uptake of the pathogen and includes inhibition of phagosome maturation. The latter refers to the pathogen's ability to protect itself from such antimicrobial host cell defenses such as ROS or copper toxicity.

Inhibition of phagosome maturation during uptake of pathogenic mycobacteria by macrophages or neutrophils has been shown to be mediated by various pathogen-derived virulence factors including the phosphatase SapM (Vergne et al., 2005), the phosphatase PtpA (Bach et al., 2008), the nucleoside diphosphate kinase Ndk (Sun et al., 2010), and ManLAM (Fratti et al., 2003). The main event in phagosome maturation is the phagosome-lysosome fusion, a step that further acidifies the resulting mature phagolysosome and delivers hydrolytic enzymes that attack the internalized pathogen. Another important feature of the maturation process is the production of ROS through the recruitment and activation of the NADPH oxidase NOX2. However, production of ROS by phagocytic cells interacting with and internalizing pathogenic mycobacteria is well established and has been shown to occur in host derived neutrophils and cultured macrophages (Deffert et al., 2014; Romero et al., 2012; Denis, 1991; May and Spagnuolo, 1987; Gordon et al., 1980). Chronic granulomatous disease (CGD) patients exhibit a genetic defect in NOX2 and generally display increased susceptibility to microbial infections. In a mouse model of CGD, host defenses has been shown to be impaired during exposure to *M. avium* (Fujita et al., 2010).

Intracellular pathogens may elaborate a variety of virulence factors with specific roles in protecting the pathogen against microbicidal host-derived products. Recently, MmcO has been shown to protect the pathogen from toxic levels of copper as the ΔmmcO mutant showed reduced resistance to the microbicidal effects of phagocytosis (Rowland and Niederweis, 2013). Surface-localized or secreted enzymes that may scavenge produced ROS may also contribute to resistance of the pathogen. *M. tuberculosis* produces the catalase-peroxidase KatG, an enzyme capable of transforming H_2O_2 to harmless products. Growth of a ΔkatG mutant of *M. tuberculosis* in macrophages from a C57Bl/6 and

NOS2-/- was shown to be impaired as compared to the parent strain (Ng et al., 2004). Our observations that MmcO is capable of scavenging ROS produced by cultured macrophages show that this membrane-anchored enzyme may be involved not only in copper transport but also in scavenging ROS during phagocytic uptake of the pathogen and thus contributing to its resistance to microbicidal activity of the macrophage. The homologous multicopper oxidase CueO of *Salmonella enterica* serovar typhimurium has been shown to be required for systemic virulence in a murine model of infection (Achard et al., 2010). The ferroxidase activity of MmcO also implicates this enzyme as playing a role in iron metabolism and uptake. Multicopper oxidases with ferroxidase activity from various organisms have been shown to contribute to iron uptake and metabolism and include hephaestin (Petrak and Vyoral, 2005), ceruplasmin (Jiang et al., 2016), and *Pseudomonas aeruginosa* MCO (Huston et al., 2002).

Funding

None to declare.

Transparency declarations

None to declare.

Declaration of Competing Interest

The authors report no conflicts of interest.

CRediT authorship contribution statement

Eyad Kinkar: Conceptualization, Methodology, Investigation, Writing - original draft. **Ayat Kinkar:** Conceptualization, Methodology, Validation. **Mazen Saleh:** Formal analysis, Writing - review & editing, Supervision, Project administration.

References

Achard, M.E., Tree, J.J., Holden, J.A., Simpfendorfer, K.R., Wijburg, O.L., et al., 2010. The multi-copper-ion oxidase CueO of *Salmonella enterica* serovar Typhimurium is required for systemic virulence. Infect. Immun. 78, 2312–2319.

Assumpção, T.C.F., Ma, D., Schwarz, A., Reiter, K., Santana, J.M., et al., 2013. Salivary antigen-5/CAP family members are Cu2+-dependent antioxidant enzymes that scavenge O2−. and inhibit collagen-induced platelet aggregation and neutrophil oxidative burst. J. Biol. Chem. 288, 14341–14361. https://doi.org/10.1074/jbc.M113.466995.

Bach, H., Papavinasasundaram, K.G., Wong, D., Hmama, Z., Av-Gay, Y., 2008. *Mycobacterium tuberculosis* virulence is mediated by PtpA dephosphorylation of human vacuolar protein sorting 33B Cell. Host Microbe 3, 316–322.

Bonomi, F., Kurtz Jr., D.M., Cui, X., 1996. Ferroxidase activity of recombinant *Desulfovibrio vulgaris* rubrerythrin. J. Biol. Inorg. Chem. 1, 67–72.

Corpet, F., 1988. Multiple sequence alignment with hierarchical clustering. Nucleic Acids Res. 16, 10881–10890.

Deffert, C., Cachat, J., Krause, K.H., 2014. Phagocyte NADPH oxidase, chronic granulomatous disease and mycobacterial infections. Cell. Microbiol. 16, 1168–1178.

Denis, M., 1991. Tumor necrosis factor and granulocyte macrophage-colony stimulating factor stimulate human macrophages to restrict growth of virulent *Mycobacterium avium* and to kill avirulent *M. avium*: killing effector mechanism depends on the generation of reactive nitrogen intermediates. J. Leukoc. Biol. Suppl. 49, 380–387.

Dick, G.J., Podell, S., Johnson, H.A., Rivera-Espinoza, Y., Bernier-Latmani, R., et al., 2008. Genomic insights into Mn (II) oxidation by the marine alphaproteobacterium *Aurantimonas* sp. strain SI85-9A1. Appl. Enviro. Microbiol. 74, 2646–2658.

Fratti, R.A., Chua, J., Vergne, I., Deretic, V., 2003. *Mycobacterium tuberculosis* glycosylated phosphatidylinositol causes phagosome maturation arrest. Proc. Natl. Acad. Sci. U. S. A. 100, 5437–5442.

Frieden, E., Hsieh, H.S., 1976. In: In: Yasunobu, K.T., Mower, H.F. (Eds.), In Iron and Copper Proteins 74. Plenum Publishing Corp, New York, pp. 89–244.

Fujita, M., Harada, E., Matsumoto, T., Mizuta, Y., Ikegame, S., et al., 2010. Impaired host defence against *Mycobacterium avium* in mice with chronic granulomatous disease. Clin. Exp. Immunol. 160, 457–460.

Gordon, A.H., Hart, P.D., Young, M.R., 1980. Ammonia inhibits phagosome–lysosome fusion in macrophages. Nature 286, 79–80. https://doi.org/10.1038/286079a0.

Grass, G., Rensing, C., 2001. CueO is a multi-copper oxidase that confers copper tolerance in *Escherichia coli*. Biochem. Biophys. Res. Commun. 286, 902–908.

Haas, J., Roth, S., Arnold, K., Kiefer, F., Schmidt, T., et al., 2013. The Protein Model Portal - a comprehensive resource for protein structure and model information. Database bat031.

Hassett, R.F., Yuan, D.S., Kosman, D.J., 1998. Spectral and kinetic properties of the Fet3 protein from *Saccharomyces cerevisiae*, a multinuclear copper ferroxidase enzyme. J. Biol. Chem. 273, 23274–23282.

Hmama, Z., Peña-Díaz, S., Joseph, S., Av-Gay, Y., 2015. Immunoevasion and immunosuppression of the macrophage by *Mycobacterium tuberculosis*. Immunol. Rev. 264, 220–232.

Huston, W.M., Jennings, M.P., McEwan, A.G., 2002. The multicopper oxidase of *Pseudomonas aeruginosa* is a ferroxidase with a central role in iron acquisition. Mol. Microbiol. 45, 1741–1750.

Jiang, B., Liu, G., Zheng, J., Chen, M., Maimaitiming, Z., et al., 2016. Hephaestin and ceruloplasmin facilitate iron metabolism in the mouse kidney. Sci. Rep. 6.

Kim, C., Lorenz, W.W., Hoopes, J.T., Dean, J.F., 2001. Oxidation of phenolate siderophores by the multicopper oxidase encoded by the *Escherichia coli* yacK gene. J. Bacteriol. 183, 4866–4875.

Longhi, G., Hanifi-Moghaddam, P., Touabassy, R., Saleh, M., 2016. Macrophage infection by mycobacteria. Mycobact. Dis. 6, 2161.

May, M.E., Spagnuolo, P.J., 1987. Evidence for activation of a respiratory burst in the interaction of human neutrophils with *Mycobacterium tuberculosis*. Infect. Immun. 55, 2304–2307.

Messerschmidt, A., Huber, R., 1990. The blue oxidases, ascorbate oxidase, laccase and ceruloplasmin modelling and structural relationships. Eur. J. Clin. Chem. Clin. Biochem. 187, 341–352. https://doi.org/10.1111/j.1432-1033.1990.tb15311.x.

Ng, V.H., Cox, J.S., Sousa, A.O., MacMicking, J.D., McKinney, J.D., 2004. Role of KatG catalase-peroxidase in mycobacterial pathogenesis: countering the phagocyte oxidative burst. Mol. Microbiol. 52, 1291–1302.

Park, Y.S., Suzuki, K., Taniguchi, N., Gutteridge, J.M., 1999. Glutathione peroxidase like activity of caeruloplasmin as an important lung antioxidant. FEBS Lett. 458, 133–136.

Petrak, J., Vyoral, D., 2005. Hephaestin-a ferroxidase of cellular iron export. Intl. J. Biochem. Cell Biol. 37, 1173–1178.

Romero, M.M., Balboa, L., Basile, J.I., López, B., Ritacco, V., et al., 2012. Clinical isolates of *Mycobacterium tuberculosis* differ in their ability to induce respiratory burst and apoptosis in neutrophils as a possible mechanism of immune escape. Clin. Dev. Immunol. 2012.

Rose, A.S., Hildebrand, P.W., 2015. NGL viewer: a web application for molecular visualization. Nucleic Acids Res. 43, 576–579. https://doi.org/10.1093/nar/gkv402.

Rowland, J.L., Niederweis, M., 2013. A multicopper oxidase is required for copper resistance in *Mycobacterium tuberculosis*. J. Bacteriol. 195, 3724–3733.

Rudolph, R., Lilie, H., 1996. In vitro refolding of inclusion body proteins. FASEB J. 10, 49–56.

Sakurai, T., Kataoka, K., 2007. Basic and applied features of multicopper oxidases, CueO, bilirubin oxidase, and laccase. Chem. Rec. 7, 220–229.

Shiva, S., Wang, X., Ringwood, L.A., Xu, X., Yuditskaya, S., et al., 2006. Ceruloplasmin is a NO oxidase and nitrite synthase that determines endocrine NO homeostasis. Nat. Chem. Biol. 2, 486–493.

Silva, C.S., Durão, P., Fillat, A., Lindley, P.F., Martins, L.O., Bento, I., 2012. Crystal structure of the multicopper oxidase from the pathogenic bacterium *Campylobacter jejuni* CGUG11284: characterization of a metallo-oxidase. Metallomics 4, 37–47.

Sun, J., Wang, X., Lau, A., Liao, T.Y., Bucci, C., Hmama, Z., 2010. Mycobacterial nucleoside diphosphate kinase blocks phagosome maturation in murine RAW 264.7 macrophages. PLoS One 5, e8769.

Tree, J.J., Ulett, G.C., Hobman, J.L., Constantinidou, C., Brown, N.L., et al., 2007. The multicopper oxidase (CueO) and cell aggregation in *Escherichia coli*. Environ. Microbiol. 9, 2110–2116. https://doi.org/10.1111/j.1462-2920.2007.01320.x.

Vasil'ev, V.B., Kachurin, A.M., Soroka, N.V., 1988. Dismutation of superoxide radicals by ceruloplasmin - details of the mechanism. Biokhimiia 53, 2051–2058.

Vergne, I., Chua, J., Lee, H.H., Lucas, M., Belisle, J., Deretic, V., 2005. Mechanism of phagolysosome biogenesis block by viable *Mycobacterium tuberculosis*. Proc. Natl. Acad. Sci. U. S. A. 102, 4033–4038.

Walev, I., Bhakdi, S.C., Hofmann, F., Djonder, N., Valeva, A., et al., 2001. Delivery of proteins into living cells by reversible membrane permeabilization with streptolysin-O. Proc. Natl. Acad. Sci. U. S. A. 98, 3185–3190.

Young, S.N., Curzon, G., 1972. A method for obtaining linear reciprocal plots with caeruloplasmin and its application in a study of the kinetic parameters of caeruloplasmin substrates. Biochem. J. 129, 273–283.